SUPPLEMENTAL INFORMATION

SUPPLEMENTAL RESULTS

CEP55 Interactions are Not Required for HIV-1 Budding

As CEP55 bound both TSG101 and ALIX, the two known cellular Gag binding partners involved in HIV-1 budding, we tested whether CEP55 was required for HIV-1 release and infectivity. siRNA depletion of CEP55 inhibited cell growth (Sakai et al., 2006), and viral Gag protein expression (not shown), which prohibited us from meaningfully testing the effects of CEP55 depletion on virus budding. We therefore instead tested whether TSG101 and ALIX mutations that abrogated CEP55 binding also inhibited HIV-1 release and infectivity.

As shown in Fig. S4A, a mutant siRNA-resistant TSG101 protein that lacked CEP55 binding activity ($TSG101_{154\text{-}164A}$) rescued HIV-1 infectivity to nearly the same extent as wild type TSG101 in cells depleted of endogenous TSG101 (compare lanes 1-3). The $TSG101_{154\text{-}164A}$ mutant also rescued other defects characteristic of inhibited virus budding, including virion release (upper right panel, compare lanes 1 and 3) and the delayed Gag processing that led to cellular accumulation of $p25^{Gag}$ and $p41^{Gag}$ cleavage intermediates (middle panel). As expected, the wild type TSG101 protein also rescued all of these budding defects, whereas a control mutant TSG101 protein that lacked PTAP binding activity ($TSG101_{M95A}$) did not.

Analogous experiments demonstrated that a mutant ALIX protein that lacked CEP55 binding activity ($ALIX_{800\text{-}802A}$) also supported HIV-1 budding. These experiments employed a mutant HIV-1 construct that lacked the ability to recruit TSG101 ($HIV\text{-}1_{\Delta PTAP}$) and therefore required ALIX protein overexpression for release and infectivity (Fisher et al., 2007; Usami et al., 2007). As shown in Fig. S4B, $HIV\text{-}1_{\Delta PTAP}$ release and infectivity were strongly stimulated by overexpression of $ALIX_{800\text{-}802A}$ (21-fold increase in infectivity), to levels that were nearly the

same as those seen for overexpression of wild type ALIX (24-fold increase). We therefore conclude that CEP55 interactions with TSG101/ESCRT-I and ALIX are not required for HIV-1 budding and infectivity, arguing against a role for CEP55 in virus release.

SUPPLEMENTAL REFERENCES

Fisher, R.D., Chung, H.Y., Zhai, Q., Robinson, H., Sundquist, W.I. and Hill, C.P. (2007) Structural and Biochemical Studies of ALIX/AIP1 and Its Role in Retrovirus Budding. *Cell*, **128**, 841-852.

Garrus, J.E., von Schwedler, U.K., Pornillos, O.W., Morham, S.G., Zavitz, K.H., Wang, H.E., Wettstein, D.A., Stray, K.M., Cote, M., Rich, R.L., Myszka, D.G. and Sundquist, W.I. (2001) Tsg101 and the vacuolar protein sorting pathway are essential for HIV-1 budding. *Cell*, **107**, 55-65.

Onishi, M., Kinoshita, S., Morikawa, Y., Shibuya, A., Phillips, J., Lanier, L.L., Gorman, D.M., Nolan, G.P., Miyajima, A. and Kitamura, T. (1996) Applications of retrovirus-mediated expression cloning. *Exp Hematol*, **24**, 324-329.

Sakai, M., Shimokawa, T., Kobayashi, T., Matsushima, S., Yamada, Y., Nakamura, Y. and Furukawa, Y. (2006) Elevated expression of C10orf3 (chromosome 10 open reading frame 3) is involved in the growth of human colon tumor. *Oncogene*, **25**, 480-486.

Usami, Y., Popov, S. and Gottlinger, H.G. (2007) Potent Rescue of Human Immunodeficiency Virus Type 1 Late Domain Mutants by ALIX/AIP1 Depends on Its CHMP4 Binding Site. *J Virol*, **81**, 6614-6622.

Welsch, S., Habermann, A., Jager, S., Muller, B., Krijnse-Locker, J. and Krausslich, H.G. (2006) Ultrastructural analysis of ESCRT proteins suggests a role for endosome-associated tubular-vesicular membranes in ESCRT function. *Traffic*, **7**, 1551-1566.

SUPPLEMENTAL TABLES

Table S1. Summary of Two Hybrid Screening Interactions

Bait	Prey	Occurrences	Implied Binding Sites
TSG101	**CEP55**		
50-390	73-419		
50-390	77-309		
50-390	151-286		
140-270	64-289	11	TSG101 (140-270), CEP55 (151-243)
140-270	66-243		
140-270	77-309		
140-270	96-301		
140-270	151-186		
ALIX	**CEP55**		
601-868	77-206	13	ALIX (601-886), CEP55 (77-206)
601-868	77-302		
601-868	77-309		
TSG101	**IQGAP1**		
240-390	1299-1555		
240-390	1308-1606		
240-390	1392-1657		
240-390	1403-1554		
240-390	1404-1553	18	TSG101 (240-390), IQGAP1 (1463-1547)
240-390	1406-1547		
240-390	1408-1605		
240-390	1413-1567		
240-390	1419-1657		
240-390	1439-1565		
240-390	1439-1567		
240-390	1463-1568		
TSG101	**ROCK1**		
231-390	462-617	2	TSG101 (231-390), ROCK1 (462-617)

Table S2. Mammalian Expression Vectors

Plasmid Name	Internal ID	Backbone	Cloning Sites	Epitope Tags	Source
pCAG.Myc	WISP06-64			N,Myc	[1]
pCAG.OSF	WISP06-65	pCAG.Myc		N,One-STrEP-FLAG	[2]
pEF.FLAG	WISP07-59	pEF4/Myc-His A		N,FLAG	Invitrogen
pcDNA.Myc.His.A(-)	WISP02-257			C,Myc- HIS	Invitrogen
pcDNA.FOS	WISP07-19	pcDNA.Myc.His.A(-)		C,FLAG-One-STrEP	Invitrogen
pCI.FLAG.NdeBam	WISP02-31	pCI-neo		N,FLAG	Promega
pEGFP-C1	WISP98-114			N,GFP	BD Bioscience
pMIH	WISP07-125	pMX-IRES-GFP			gift from Dr.Sugamura
pGag-Pol	WISP07-127				gift from Dr.Sugamura
pMD.G	WISP03-279				gift from Dr.Trono
pEF.FLAG.ALIX	WISP07-20	pEF.FLAG	EcoRI, BamHI	N,FLAG	BC020066 [3]
pEF.FLAG.ALIX.794-796A	WISP07-21	pEF.FLAG	EcoRI, BamHI	N,FLAG	BC020066 [3]
pEF.FLAG.ALIX.800-802A	WISP07-22	pEF.FLAG	EcoRI, BamHI	N,FLAG	BC020066 [3]
pcDNA.ALIX.MycHIS	WISP03-344	pcDNA.myc.His.A(-)	EcoRI, BamHI	C,Myc-HIS	[4]
pEGFP.ALIX	WISP07-23	pEGFP.C1	EcoRI, BamHI	N,GFP	BC020066 [3]
pCI.FLAG.ALIX	WISP03-345	pCI.FLAG.NdeBam	NdeI, BamHI	N,FLAG	[5]
pCI.FLAG.ALIX.I212D	WISP05-117	pCI.FLAG.NdeBam	NdeI, BamHI	N,FLAG	[5]
pCI.FLAG.ALIX.F676D	WISP06-164	pCI.FLAG.NdeBam	NdeI, BamHI	N,FLAG	[5]
pCI.FLAG.ALIX.800-802A	WISP07-24	pCI.FLAG.NdeBam	NdeI, BamHI	N,FLAG	[5]
pCI.FLAG.ALIX.744,745A	WISP07-71	pCI.FLAG.NdeBam	NdeI, BamHI	N,FLAG	[5]
pcDNA.CEP55.mycHIS	WISP07-25	pcDNA.myc.His.A(-)	XbaI, EcoRI	C, Myc-HIS	BC008947 [3]
pcDNA.CEP55.FOS	WISP07-26	pcDNA.FOS	XbaI, EcoRI	C,FLAG-One-STrEP	BC008947 [3]
pCAG.OSF.CEP55	WISP07-27	pCAG.OSF	KpnI, XhoI	N,One-STrEP-FLAG	BC008947 [3]
pCAG.OSF.TSG101	WISP06-67	pCAG.OSF	KpnI, XhoI	N,One-STrEP-FLAG	[2]
pCAG.Myc.TSG101	WISP06-66	pCAG.Myc	KpnI, XhoI	N,Myc	[2]
pCAG.Myc.TSG101.154-164A	WISP07-28	pCAG.Myc	KpnI, XhoI	N,Myc	HeLa cDNA
pcDNA.GFP.TSG101	WISP02-22	pcDNA	KpnI, BamHI	N,GFP	Myriad Genetics
pCAG.NT.VPS28	WISP06-70	pCAG	(KpnI), XhoI	none	[2]
pCAG.Myc.VPS28	WISP06-71	pCAG.Myc	KpnI, XhoI	N,Myc	[2]
pCAG.NT.VPS37B	WISP06-76	pCAG	(KpnI), XhoI	none	[2]
pCAG.Myc.VPS37B	WISP06-77	pCAG.Myc	KpnI, XhoI	N,Myc	[2]
pCAG.Myc.VPS37C	WISP06-82	pCAG.Myc	KpnI, XhoI	N,Myc	[2]
pcDNA.NT.EI4A (MVB12A)	WISP06-87	pcDNA.myc.His.A(-)	XbaI, EcoRI	none	[2]
pCAG.Myc.EI4A. (MVB12A)	WISP06-88	pCAG.Myc	KpnI, XhoI	N,Myc	[2]
pcDNA.CHMP2A.FLAG	WISP02-337	pcDNA.myc.His.A(-)	EcoRI, BamHI	C,FLAG	[6]
pcDNA.CHMP4B.FLAG	WISP02-338	pcDNA.myc.His.A(-)	EcoRI, BamHI	C,FLAG	[6]
pcDNA.CHMP5.FLAG	WISP02-339	pcDNA.myc.His.A(-)	EcoRI, BamHI	C,FLAG	[6]
pCAG.OSF.CHMP6	WISP07-29	pCAG.OSF	KpnI, XhoI	N,One-STrEP-FLAG	BC010108 [3]
pCAG.Myc.ROCK1	WISP07-30	pCAG.Myc	KpnI, XhoI	N,Myc	[7]
pCAG.Myc.CD2AP	WISP07-31	pCAG.Myc	KpnI, XhoI	N,Myc	AF164377 [3]
pCAG.OSF.CD2AP	WISP07-32	pCAG.OSF	KpnI, XhoI	N,One-STrEP-FLAG	AF164377 [3]
pEGFP.VPS4A.WT	WISP01-111	pEGFP-C1	EcoRI, BamHI	N,GFP	[4]
pEGFP.VPS4A.K173Q	WISP01-112	pEGFP-C1	EcoRI, BamHI	N,GFP	[4]
pMIH.FLAG.ALIX	WISP07-126	pMIH	BamHI, EcoRI	N,FLAG	BC020066 [3]

[1] Madaule P, Eda M, Watanabe N, Fujisawa K, Matsuoka T, Bito H, Ishizaki T, Narumiya S.(1998) Role of citron kinase as a target of the small GTPase Rho in cytokinesis. Nature. 394:491-494.
[2] Morita E, Sandrin V, Alam SL, Eckert DM, Gygi SP, Sundquist WI. (2007) Identification of the human MVB12 proteins as ESCRT-I subunits that function in HIV budding. Cell Host & Microbe 2: 41-53.
[3] EST clone number from ATCC.
[4] von Schwedler UK, Stuchell M, Muller B, Ward DM, Chung HY, Morita E, Wang HE, Davis T, He GP, Cimbora DM, Scott A, Krausslich HG, Kaplan J, Morham SG, Sundquist WI. (2003) The protein network of HIV budding. Cell. 114:701-713.
[5] Fisher RD, Chung HY, Zhai Q, Robinson H, Sundquist WI, Hill CP. (2007) Structural and biochemical studies of ALIX/AIP1 and its role in retrovirus budding. Cell. 128: 841-852.
[6] Ward DM, Vaughn MB, Shiflett SL, White PL, Pollock AL, Hill J, Schnegelberger R, Sundquist WI, Kaplan J. (2005) The role of LIP5 and CHMP5 in multivesicular body formation and HIV-1 budding in mammalian cells. J Biol Chem. 280:10548-10555.
[7] Ishizaki T, Naito M, Fujisawa K, Maekawa M, Watanabe N, Saito Y, Narumiya S. (1997) p160ROCK, a Rho-associated coiled-coil forming protein kinase, works downstream of Rho and induces focal adhesions. FEBS Lett. 404:118-124.

Table S3. Yeast Two hybrid Vectors

Plasmid Name	Internal ID	Backbone	Cloning Sites	Fusion Proteins	Source
pGADT7	WISP03-38			N, GAL4 AD	BD Bioscience
pGADT7.TSG101.WT	WISP03-186	pGADT7	NcoI, BamHI	N, GAL4 AD	[1]
pGADT7.TSG101.M95A	WISP03-240	pGADT7	NcoI, BamHI	N, GAL4 AD	[1]
pGADT7.TSG101.ΔPTAP	WISP04-128	pGADT7	EcoRI, BamHI	N, GAL4 AD	HeLa cDNA
pGADT7.TSG101.1-145	WISP04-308	pGADT7	EcoRI, BamHI	N, GAL4 AD	[2]
pGADT7.TSG101.146-311	WISP04-310	pGADT7	EcoRI, BamHI	N, GAL4 AD	[2]
pGADT7.TSG101.312-390	WISP04-312	pGADT7	EcoRI, BamHI	N, GAL4 AD	[2]
pGADT7.TSG101.231-329	WISP07-33	pGADT7	EcoRI, BamHI	N, GAL4 AD	HeLa cDNA
pGADT7.TSG101.146-235	WISP07-34	pGADT7	EcoRI, BamHI	N, GAL4 AD	HeLa cDNA
pGADT7.TSG101.164-235	WISP07-35	pGADT7	EcoRI, BamHI	N, GAL4 AD	HeLa cDNA
pGADT7.TSG101.182-235	WISP07-36	pGADT7	EcoRI, BamHI	N, GAL4 AD	HeLa cDNA
pGADT7.TSG101.200-235	WISP07-37	pGADT7	EcoRI, BamHI	N, GAL4 AD	HeLa cDNA
pGADT7.TSG101.218-235	WISP07-38	pGADT7	EcoRI, BamHI	N, GAL4 AD	HeLa cDNA
pGADT7.TSG101.149-151A	WISP07-39	pGADT7	EcoRI, BamHI	N, GAL4 AD	HeLa cDNA
pGADT7.TSG101.152-154A	WISP07-40	pGADT7	EcoRI, BamHI	N, GAL4 AD	HeLa cDNA
pGADT7.TSG101.155-157A	WISP07-41	pGADT7	EcoRI, BamHI	N, GAL4 AD	HeLa cDNA
pGADT7.TSG101.158-160A	WISP07-42	pGADT7	EcoRI, BamHI	N, GAL4 AD	HeLa cDNA
pGADT7.TSG101.161-163A	WISP07-43	pGADT7	EcoRI, BamHI	N, GAL4 AD	HeLa cDNA
pGADT7.ROCK1	WISP03-289	pGADT7	NdeI, XmaI	N, GAL4 AD	[3]
pGADT7.ALIX.WT	WISP03-238	pGADT7	NdeI, BamHI	N, GAL4 AD	[1]
pGADT7.ALIX.1-868	WISP03-333	pGADT7	NdeI, BamHI	N, GAL4 AD	BC020066 [4]
pGADT7.ALIX.1-716	WISP03-334	pGADT7	NdeI, BamHI	N, GAL4 AD	BC020066 [4]
pGADT7.ALIX.1-628	WISP03-335	pGADT7	NdeI, BamHI	N, GAL4 AD	BC020066 [4]
pGADT7.ALIX.1-473	WISP03-336	pGADT7	NdeI, BamHI	N, GAL4 AD	BC020066 [4]
pGADT7.ALIX.1-297	WISP03-337	pGADT7	NdeI, BamHI	N, GAL4 AD	BC020066 [4]
pGADT7.ALIX.1-167	WISP03-338	pGADT7	NdeI, BamHI	N, GAL4 AD	BC020066 [4]
pGADT7.ALIX.717-868	WISP07-44	pGADT7	EcoRI, BamHI	N, GAL4 AD	BC020066 [4]
pGADT7.ALIX.751-868	WISP07-45	pGADT7	EcoRI, BamHI	N, GAL4 AD	BC020066 [4]
pGADT7.ALIX.781-868	WISP07-46	pGADT7	EcoRI, BamHI	N, GAL4 AD	BC020066 [4]
pGADT7.ALIX.811-868	WISP07-47	pGADT7	EcoRI, BamHI	N, GAL4 AD	BC020066 [4]
pGADT7.ALIX.841-868	WISP07-48	pGADT7	EcoRI, BamHI	N, GAL4 AD	BC020066 [4]
pGADT7.CEP55.WT	WISP04-288	pGADT7	EcoRI, BamHI	N, GAL4 AD	BC008947 [4]
pGADT7.CEP55.19-407	WISP07-49	pGADT7	EcoRI, BamHI	N, GAL4 AD	BC008947 [4]
pGADT7.CEP55.19-385	WISP07-50	pGADT7	EcoRI, BamHI	N, GAL4 AD	BC008947 [4]
pGADT7.CEP55.157-236	WISP07-51	pGADT7	EcoRI, BamHI	N, GAL4 AD	BC008947 [4]
pGADT7.CEP55.359-464	WISP07-52	pGADT7	EcoRI, BamHI	N, GAL4 AD	BC008947 [4]
pGADT7.CEP55.408-464	WISP07-53	pGADT7	EcoRI, BamHI	N, GAL4 AD	BC008947 [4]
pGBKT7	WISP03-39			N, GAL4 DNA-BD	BD Bioscience
pGBKT7.TSG101.WT	WISP03-192	pGBKT7	NcoI, BamHI	N, GAL4 DNA-BD	[1]
pGBKT7.TSG101.M95A	WISP03-219	pGBKT7	NcoI, BamHI	N, GAL4 DNA-BD	[1]
pGBKT7.TSG101.DPTAP	WISP04-129	pGBKT7	EcoRI, BamHI	N, GAL4 DNA-BD	HeLa cDNA
pGBKT7.TSG101.1-145	WISP04-307	pGBKT7	EcoRI, BamHI	N, GAL4 DNA-BD	[2]
pGBKT7.TSG101.146-311	WISP04-309	pGBKT7	EcoRI, BamHI	N, GAL4 DNA-BD	[2]
pGBKT7.TSG101.312-390	WISP04-311	pGBKT7	EcoRI, BamHI	N, GAL4 DNA-BD	[2]
pGBKT7.IQGAP1.1463-1547	WISP04-29	pGBKT7	NdeI, SalI/ XhoI	N, GAL4 DNA-BD	KIAA0051 [5]
pGBKT7.CEP55.WT	WISP04-289	pGBKT7	EcoRI, BamHI	N, GAL4 DNA-BD	BC008947 [4]
pGBKT7.CEP55.19-407	WISP07-54	pGBKT7	EcoRI, BamHI	N, GAL4 DNA-BD	BC008947 [4]
pGBKT7.CEP55.19-385	WISP07-55	pGBKT7	EcoRI, BamHI	N, GAL4 DNA-BD	BC008947 [4]
pGBKT7.CEP55.157-236	WISP07-56	pGBKT7	EcoRI, BamHI	N, GAL4 DNA-BD	BC008947 [4]
pGBKT7.CEP55.359-464	WISP07-57	pGBKT7	EcoRI, BamHI	N, GAL4 DNA-BD	BC008947 [4]
pGBKT7.CEP55.408-464	WISP07-58	pGBKT7	EcoRI, BamHI	N, GAL4 DNA-BD	BC008947 [4]

[1] von Schwedler UK, Stuchell M, Muller B, Ward DM, Chung HY, Morita E, Wang HE, Davis T, He GP, Cimbora DM, Scott A, Krausslich HG, Kaplan J, Morham SG, Sundquist WI. (2003) The protein network of HIV budding. Cell. 114:701-713.
[2] Langelier C, von Schwedler UK, Fisher RD, De Domenico I, White PL, Hill CP, Kaplan J, Ward D, Sundquist WI. (2006) Human ESCRT-II complex and its role in human immunodeficiency virus type 1 release. J Virol. 80:9465-9480.
[3] Ishizaki T, Naito M, Fujisawa K, Maekawa M, Watanabe N, Saito Y, Narumiya S. (1997) p160ROCK, a Rho-associated coiled-coil forming protein kinase, works downstream of Rho and induces focal adhesions. FEBS Lett. 404:118-124.
[4] EST clone number from ATCC.
[5] EST clone number from KAZUSA DNA research institute.

Table S4. Antibodies

Name	Host	Clone #	Dilution Factor	Conjugation	Experiment	Source
Myc	mouse	9E10	1:3000	none	WB	Covance
Myc	goat	ab9132	1:1000	none	WB	Abcam
FLAG	mouse	M2	1:5000	none	WB	Sigma
FLAG	rabbit	F7425	1:1000	none	ICC	Sigma
IQGAP1	mouse	VIC1	1:1000	none	WB	MBL
HIV CA	rabbit		1:3000	none	WB	Original
HIV MA	rabbit		1:3000	none	WB	Gift from Didier Trono
TSG101	mouse	4A10	1:1000	none	WB	GeneTex
ALIX	rabbit		1:1000	none	WB	[1]
ALIX	rabbit		1:100	none	ICC	[1]
VPS4A	rabbit		1:1000	none	ICC	[2]
α-tubulin	mouse	DM1A	1:5000	none	WB	Sigma
α-tubulin	mouse	DM1A	1:1000	none	ICC	Sigma
γ-tubulin	mouse	GTU-88	1:1000	none	ICC	Sigma
rabbit IgG	donkey	A-21206	1:1000	Alexa 488	ICC	Invitrogen/ Molecular Probes
mouse IgG	goat	A-11032	1:1000	Alexa 594	ICC	Invitrogen/ Molecular Probes

WB: Western Blotting, ICC: Immunocytochemistry

[1] Fisher RD, Chung HY, Zhai Q, Robinson H, Sundquist WI, Hill CP. (2007) Structural and biochemical studies of ALIX/AIP1 and its role in retrovirus budding. Cell. 128: 841-852
[2] von Schwedler UK, Stuchell M, Muller B, Ward DM, Chung HY, Morita E, Wang HE, Davis T, He GP, Cimbora DM, Scott A, Krausslich HG, Kaplan J, Morham SG, Sundquist WI. (2003) The protein network of HIV budding. Cell. 114:701-713.

SUPPLEMENTAL FIGURE CAPTIONS

Fig. S1. CD2AP Co-precipitates with ESCRT-I and ALIX.

(**A**) OSF-CD2AP co-precipitates Myc-ALIX. OSF-CD2AP or empty vector controls were tested for co-precipitation with overexpressed Myc-ALIX. Western blots show: 1) Myc-ALIX levels in soluble lysates (middle panel, Lysate, IB: anti-Myc), 2) OSF-CD2AP bound to the StrepTactin matrix (lower panel, IP:Strep, IB:anti-FLAG), and 3) Co-precipitated Myc-ALIX (upper panel, IP:Strep, IB:anti-Myc). In this experiment, and in those shown in Figs. 1B, 2B (right) and 2C (right), 293T cells were seeded (3 x 10^6 cells/55 cm^2 dish) and co-transfected with 3 μg of each relevant expression plasmid (polyethylenimine 25,000 KDa; Polysciences, Warrington, PA) as described (Durocher et al., 2002). Cells were harvested 48h post-transfection by incubation in 300 μl lysis buffer (LB: 50mM Tris (pH 7.4), 150mM NaCl) supplemented with proteinase inhibitor cocktail (Sigma) and 1% Triton X-100. Lysates were clarified by centrifugation (18,000 x g, 10 min, 4°), and incubated with StrepTactin Sepharose (40 μl slurry, IBA GmbH, Gottingen Germany, 2h). The matrix was washed 4X in wash buffer (WB: 20 mM Tris (pH 7.4), 150 mM NaCl) supplemented with 0.1% Triton X100, and bound proteins were detected by western blotting. A list of the antibodies used in western blots is provided in Table S4.

(**B**) OSF-CD2AP co-precipitates the entire ESCRT-I complex. Western blots show: 1) ESCRT-I protein levels in soluble lysates (middle panel, Lysate, IB:anti-Myc), 2) OSF-CD2AP bound to the StrepTactin matrix (lower panel, IP:Strep, IB:anti-FLAG), and ESCRT-I proteins co-precipitated onto the matrix (upper panel, IP:Strep, IB:anti-Myc). Note that Myc-tagged versions of all four ESCRT-I subunits were co-expressed in these experiments. Samples in lanes 1 were co-transfected with an empty expression vector (negative control) and samples in lanes 2 were co-transfected with an OSF-CD2AP expression vector.

Fig. S2. CEP55 Co-precipitations with ESCRT-I and ALIX.

(**A**) OSF-CEP55 co-precipitates endogenous TSG101 and ALIX. Western blots show: Panels 2 and 4: Endogenous TSG101 and ALIX protein levels in soluble lysates (Lysate, IB:anti-TSG101 or anti-ALIX), Panel 5: OSF-CEP55 protein bound to the StrepTactin matrix (IP:Strep, IB:anti-FLAG). Panels 1 and 3: TSG101 or ALIX protein co-precipitated onto the matrix (IP:Strep, IB:anti-TSG101 or anti-ALIX). Samples in lanes 1 were transfected with an empty expression vector (negative control) and samples in lanes 2 were transfection with an OSF-CEP55 expression vector. The ALIX protein frequently appears as a doublet in Western blots (e.g., see Figs. 6 and S2A). The upper band corresponds to the full length ALIX protein, and the lower band is therefore presumably a degradation product.

(**B**) OSF-CEP55 co-precipitates the entire ESCRT-I complex. Western blots show: Middle panel: ESCRT-I protein levels in soluble lysates (Lysate, IB:anti-Myc), Lower panel: OSF-CEP55 protein bound to the StrepTactin matrix (IP:Strep, IB:anti-FLAG), and Upper Panel: ESCRT-I protein co-precipitated onto the matrix (IP: Strep, IB:anti-Myc). Note that Myc-tagged versions of all four ESCRT-I subunits were co-expressed in these experiments. Samples in lanes 1 were co-transfected with an empty expression vector (negative control) and samples in lanes 2 were co-transfected with an OSF-CEP55 expression vector.

Fig. S3. Yeast Two Hybrid Analyses of CEP55 Dimerization.

Yeast two hybrid mapping of the elements required for CEP55 dimerization. CEP55-AD fusions or control AD constructs (Empty) were co-expressed together with CEP55-DBD fusions or control DBD constructs (Empty) and tested for positive yeast two hybrid interactions (left panel) or co-transformation (right panel, control). CEP55 constructs are summarized schematically in Figure 2A. This experiment shows that full length CEP55-AD and CEP55-DBD constructs

produce a positive two hybrid interaction and that this interaction maps to CEP55 residues 19-385.

Fig. S4. CEP55 Is Not Required for HIV-1 Release and Infectivity.

(**A**) A TSG101 construct lacking CEP55 binding activity rescues HIV-1 release and infectivity from cells depleted of endogenous TSG101. In all cases, 5 x10^5 293T cells/well (6 well plates) were transfected with 1 μg R9 proviral HIV-1 expression plasmid and depleted of endogenous TSG101 (Garrus et al., 2001). The figure shows viral titers (left) and virion release (upper right) in the absence of siRNA-resistant TSG101 expression (lanes 1, negative control), or upon expression of: wild type TSG101 (lanes 2, WT TSG101, positive control), a TSG101 mutant lacking CEP55 binding activity (lane 3, $TSG101_{154\text{-}164A}$), or a TSG101 mutant lacking PTAP binding activity (lanes 4, $TSG101_{M95A}$, negative control). Virus release (upper right, Virus) was assayed by western blot detection of virion-associated MA and CA proteins. Lower right panels show cell-associated TSG101 (bottom) and viral Gag and proteolytic processing products (middle, protein labels at right). HIV-1 infections were initiated by transfection of the proviral HIV-1 R9 construct, with cell- and virion-associated Gag proteins detected by western blotting and viral titers measured using single-cycle MAGIC assays as described (Garrus et al., 2001). (**B**) An ALIX construct lacking CEP55 binding activity rescues release and infectivity of HIV-$1_{\Delta PTAP}$. All 293T cells expressed the ALIX-dependent HIV-$1_{\Delta PTAP}$ virus (Fisher et al., 2007). HIV-1 infectivity (left) and release (right) were assayed in the absence of ALIX overexpression (lanes 1, Empty, negative control), upon overexpression of wild type ALIX (lanes 2, WT ALIX, positive control) or upon overexpression of a mutant ALIX construct that lacked CEP55 binding activity (lanes 3, $ALIX_{800\text{-}802A}$). Other panels are the same as in part A. Note that these experiments were also repeated in HeLa cells with the same results (not shown).

Fig. S5. Immunofluorescence Localization of Endogenous ALIX at Flemming Bodies and Centrosomes.

Immunofluorescence and DIC images showing that γ-Tubulin (green) and endogenous ALIX (red) co-localize at the midbodies of dividing HeLa cells (upper row, arrowheads) and the centrosomes of non-dividing HeLa cells (lower row, arrowheads).

Fig. S6. CEP55 Is Required for Flemming Body Localization of TSG101/ESCRT-I and ALIX.

Double-labeled immunofluorescence and DIC images showing that siRNA depletion of CEP55 blocks midbody localization of GFP-TSG101/ESCRT-I (**A**) and GFP-ALIX (**B**) whereas siRNA depletion of TSG101 does not block midbody localization of FLAG-CEP55 (**C**). Similarly, ALIX depletion does not block midbody localization of FLAG-CEP55 (**D**) or GFP-TSG101 (**E**).

(**A**) Lack of GFP-TSG101/ESCRT-I (0.5 μg GFP-TSG101, VPS28, VPS37B, and MVB12A DNA) localization at the midbodies of dividing HeLa cells depleted of CEP55. This experiment, and those in parts (B)-(E) followed the time course: t=0, cells seeded at 4 x 10^5 cells/well; t=24 h, protein expression vector transfected (0.5 μg DNA, Lippofectamine, Invitrogen); t=48 h, cells trypsin treated and reseeded with 4-16 fold dilution onto 12 well glass plates; t=72 h, siRNA transfection (Lipofectamin RNAi MAX); t=78 h, media changed + siRNA transfected; t=96 h, siRNA transfected, t=102h, media changed, t=120h, cells fixed, stained, and imaged. Microtubule staining (red, α-Tubulin) is shown here is shown in columns 1, 3, and 5 for reference, and expanded views of the midbodies are shown in column 5.

(**B**) Lack of GFP-ALIX (0.5 μg DNA) localization to the midbodies of dividing cells depleted of CEP55.

(**C**) FLAG-CEP55 (0.5 μg DNA) localization at the midbodies of dividing cells depleted of TSG101.

(**D**) FLAG-CEP55 (0.5 μg DNA) localization at the midbodies of dividing cells depleted of ALIX.

(**E**) GFP-TSG101/ESCRT-I (0.125 μg each of GFP-TSG101, VPS28, VPS37B, and MVB12A DNA) localization at the midbodies of dividing cells depleted of ALIX.

Fig. S7. CEP55 Depletion Quantitatively Blocks ALIX Localization to Midbodies.

Transduced HeLa cells expressing FLAG-ALIX were depleted of CEP55 or treated with a control siRNA, and cells undergoing cytokinesis were scored for the presence or absence of FLAG-ALIX at the midbody. FLAG-ALIX expressing HeLa cells were created using a MuLV-based retroviral vector, (pMIH, derived from pMX-IRES-GFP (Onishi et al., 1996)), that expressed FLAG-ALIX and also expressed the murine H2KK protein from an IRES sequence. Vector stocks were created by co-transfecting pMIH-FLAG-ALIX (6 μg) with pGag-pol (4 μg, (Onishi et al., 1996)), and pMD.G envelope (2 μg, (Onishi et al., 1996)) into 293T cells (3 x 10^6 cells/10cm plate) using Polyethyleneimine (PEI). 36 h post-transfection, vector-containing supernatants were harvested and filtered (0.22 μm, Millipore). HeLa cells (2 x 10^6 cells/10 cm plate) were then incubated for 12 h with 5 ml vector-containing supernatants together with polybrene (8ug/ml) for 12h. After an additional 24 h, HeLa cells were trypsinized and transduced cells were bound to magnetic beads conjugated with anti-H2KK antibody and magnetically purified (Militenyi Biotec, Germany). >95% of the purified cells expressed H2KK as measured by FACS using FITC labeled anti-H2KK antibody. The resulting FLAG-ALIX expressing cells were then replated (5 x 10^4 cells/well in a 6 well plate), transfected every 12 h (3x) with an siRNA against CEP55 or a control siRNA (10 μM, Lipofectamin RNAi Max, Invitrogen). 24 h

after the third siRNA transfection, cells were fixed, stained with anti-FLAG and anti-α-Tubulin antibodies, and scored for FLAG-ALIX localization. Measurements were performed in triplicate (n=20 midbodies from 500-1000 cells each) and error bars denote standard deviations.

Fig. S8. Endogenous VPS4A Localizes to Very Thin Midbodies.

(**A**) Double-labeled immunofluorescence images showing localization of endogenous VPS4A at the Flemming body within a very thin midbody (yellow arrowheads), but not at Flemming bodies within thicker midbodies (white arrowheads). Microtubules were also stained (α-Tubulin, red). These images are stacked confocal z slices.

(**B**) Quantification of the midbody localization of endogenous VPS4 in cells depleted of TSG101, ALIX, CEP55, or treated with an irrelevant siRNA (Control). ~20 midbodies were counted in each case.

Fig. S9. Time Lapse Movies Showing Cytokinesis Defects in Cells Depleted of Endogenous ALIX.

(**A**) Phase contrast, time lapse images of a field of HeLa cells treated with a control siRNA.

(**B**) Time lapse images of a field of ALIX-depleted HeLa cells. Note that the cells exhibit both early cytokinesis defects (i.e., rapid re-coalescence into multiploid cells following furrow ingression, yellow arrows) and late cytokinesis defects (i.e., arrested midbody formation with late re-coalescence, blue arrow).

(**C**) Time lapse image of an isolated multinuclear ALIX-depleted HeLa cell that begins to divide, forms a nearly complete cleavage furrow (t=140-160 min), and then rapidly re-coalescences into a single cell (t=180-220 min).

(**D**) Time lapse image of an isolated ALIX-depleted HeLa cell showing a late cytokinesis defect (blue arrow). Note that the midbody forms, and remains stably arrested for >9 h (t=45-865 min) before the mother and daughter re-coalescence into a single cell at ~870 min).

Fig. S10. ALIX Localizes to Class E Compartments Induced by Expression of Dominant Negative VPS4$_{K173Q}$.

(**A**) Immunofluorescence images showing localization of FLAG-ALIX (red) together with wild type VPS4A-GFP (green, top row) or the VPS4A$_{K173Q}$-GFP mutant (bottom row), which induces formation of enlarged, aberrant endosomes ("class E compartments"), and traps the ESCRT machinery on their surface. Merged images are shown in column 3, and DIC images are shown in column 4. These data are in good agreement with similar analyses by Krausslich and colleages (Welsch et al., 2006).

(**B**) Quantification of the percentage of cells in which VPS4-GFP proteins (light bars) and FLAG-ALIX (dark bars) exhibited class E localization. Left: co-expression with wild type VPS4-GFP, Right: co-expression with VPS4A$_{K173Q}$-GFP. Five fields of ~100 cells each were counted, and error bars denote standard deviations.

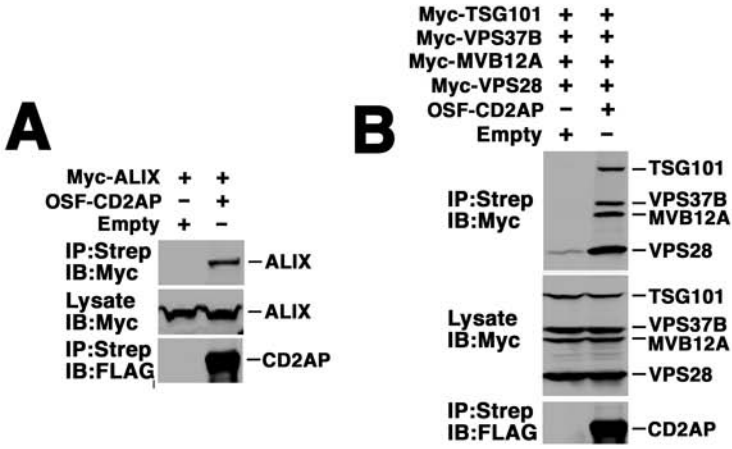
A
Myc-ALIX + +
OSF-CD2AP − +
Empty + −
IP:Strep
IB:Myc
ALIX
Lysate
IB:Myc
ALIX
IP:Strep
IB:FLAG
CD2AP
B
Myc-TSG101 + +
Myc-VPS37B + +
Myc-MVB12A + +
Myc-VPS28 + +
OSF-CD2AP − +
Empty + −
IP:Strep
IB:Myc
TSG101
VPS37B
MVB12A
VPS28
Lysate
IB:Myc
TSG101
VPS37B
MVB12A
VPS28
IP:Strep
IB:FLAG
CD2AP

Figure S2

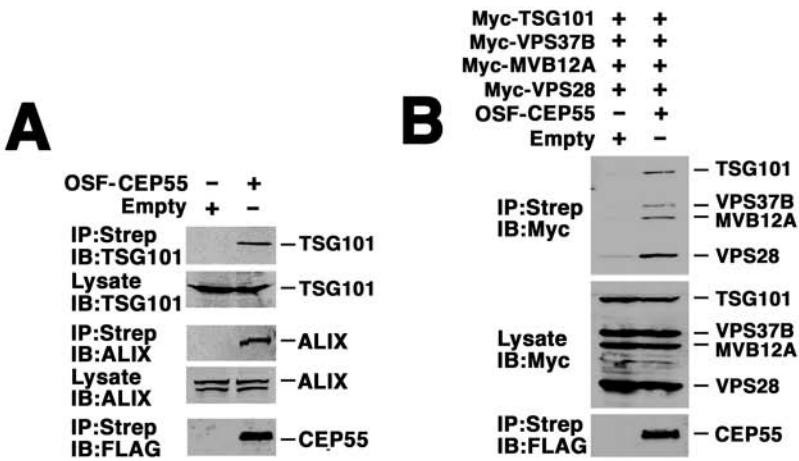
A
OSF-CEP55 − +
Empty + −
IP:Strep IB:TSG101
TSG101
Lysate IB:TSG101
TSG101
IP:Strep IB:ALIX
ALIX
Lysate IB:ALIX
ALIX
IP:Strep IB:FLAG
CEP55
B
Myc-TSG101 + +
Myc-VPS37B + +
Myc-MVB12A + +
Myc-VPS28 + +
OSF-CEP55 − +
Empty + −
IP:Strep IB:Myc
TSG101
VPS37B
MVB12A
VPS28
Lysate IB:Myc
TSG101
VPS37B
MVB12A
VPS28
IP:Strep IB:FLAG
CEP55

Figure S3

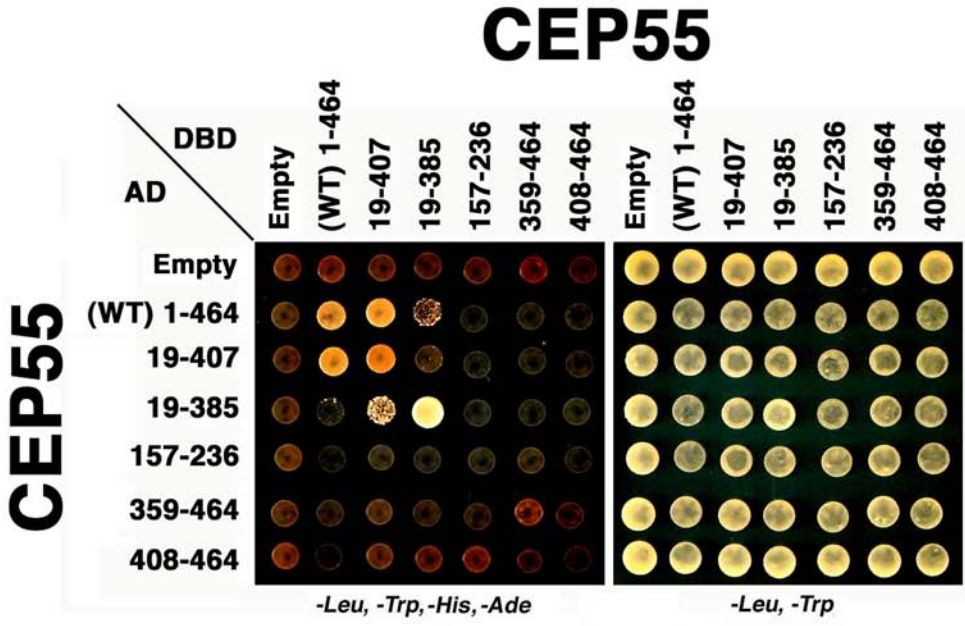
CEP55
CEP55
DBD
AD
Empty
(WT) 1-464
19-407
19-385
157-236
359-464
408-464
Empty
(WT) 1-464
19-407
19-385
157-236
359-464
408-464
Empty
(WT) 1-464
19-407
19-385
157-236
359-464
408-464
-Leu, -Trp, -His, -Ade
-Leu, -Trp

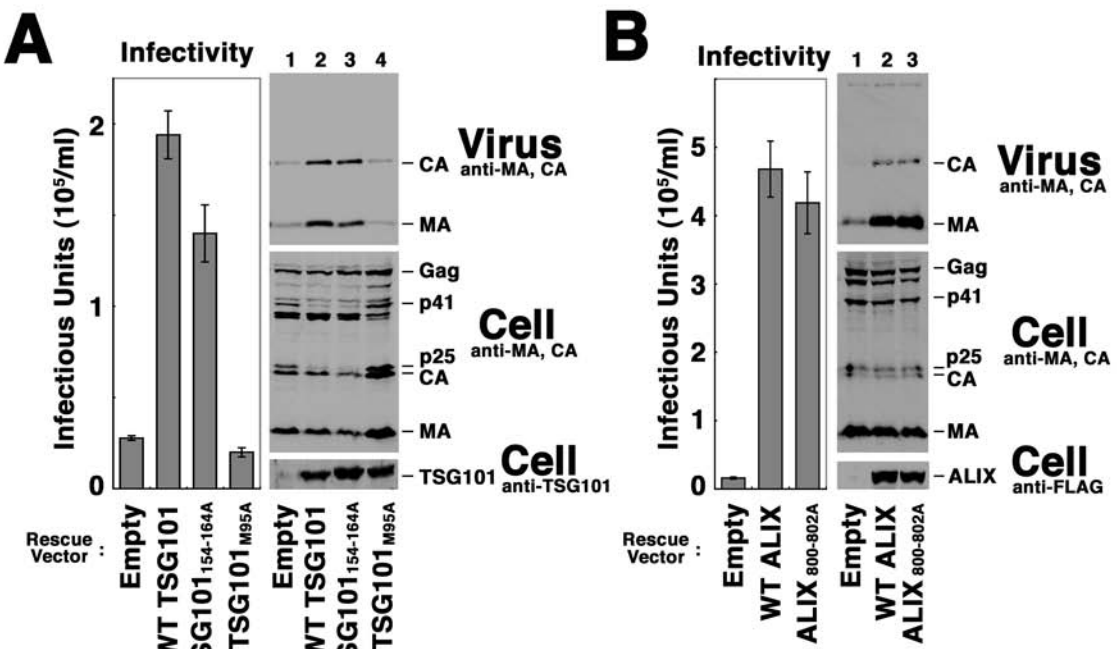
A
Infectivity
Infectious Units (10⁵/ml)
2
1
0
1 2 3 4
CA
MA
Virus
anti-MA, CA
Gag
p41
p25
CA
MA
Cell
anti-MA, CA
TSG101
Cell
anti-TSG101
Rescue Vector :
Empty
WT TSG101
TSG101 154-164A
TSG101 M95A
Empty
WT TSG101
TSG101 154-164A
TSG101 M95A
B
Infectivity
Infectious Units (10⁵/ml)
5
4
3
2
1
0
1 2 3
CA
MA
Virus
anti-MA, CA
Gag
p41
p25
CA
MA
Cell
anti-MA, CA
ALIX
Cell
anti-FLAG
Rescue Vector :
Empty
WT ALIX
ALIX 800-802A
Empty
WT ALIX
ALIX 800-802A

Figure S5

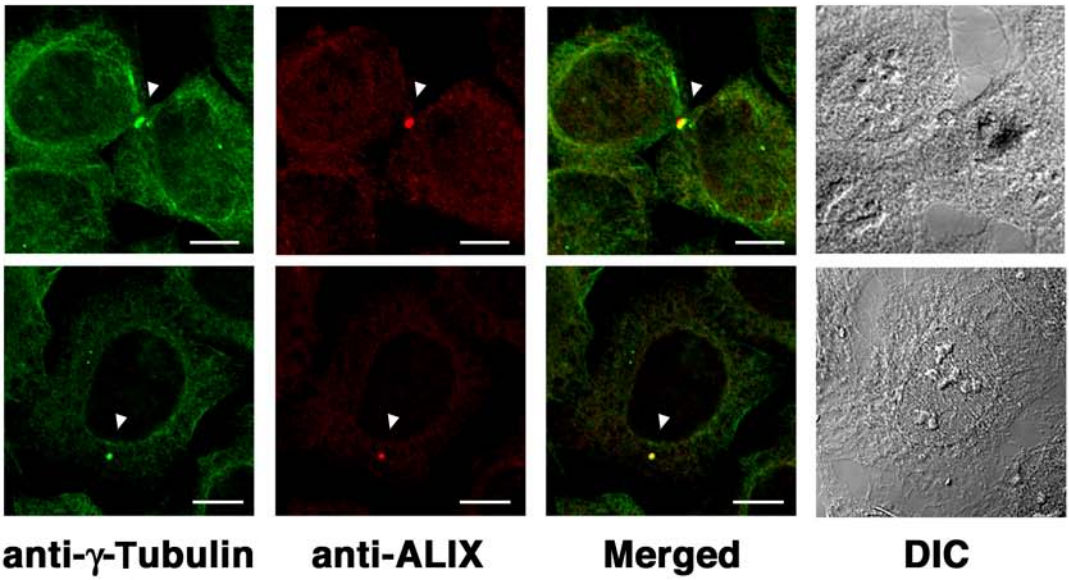

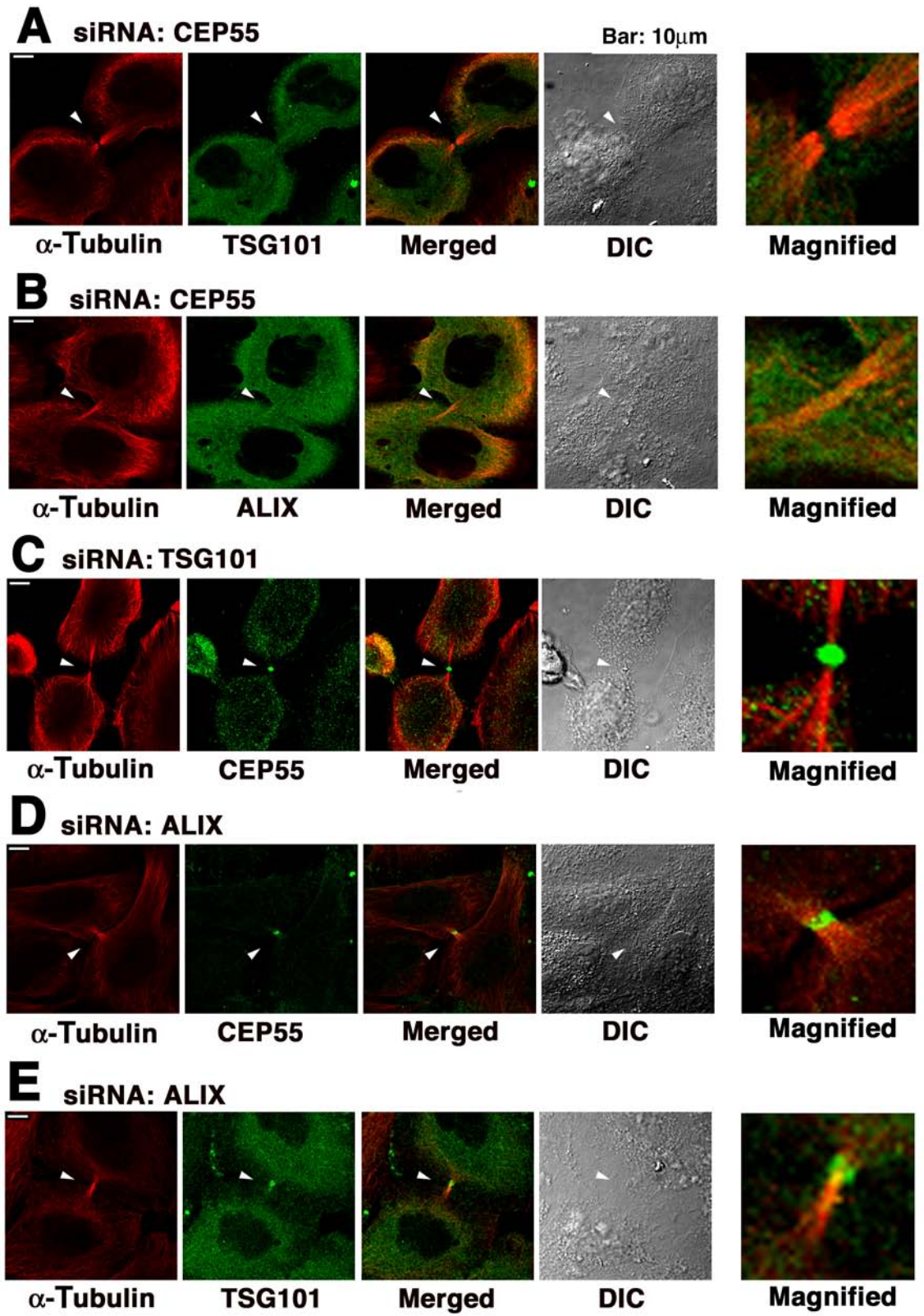
A siRNA: CEP55
Bar: 10μm
α-Tubulin
TSG101
Merged
DIC
Magnified
B siRNA: CEP55
α-Tubulin
ALIX
Merged
DIC
Magnified
C siRNA: TSG101
α-Tubulin
CEP55
Merged
DIC
Magnified
D siRNA: ALIX
α-Tubulin
CEP55
Merged
DIC
Magnified
E siRNA: ALIX
α-Tubulin
TSG101
Merged
DIC
Magnified

Figure S7

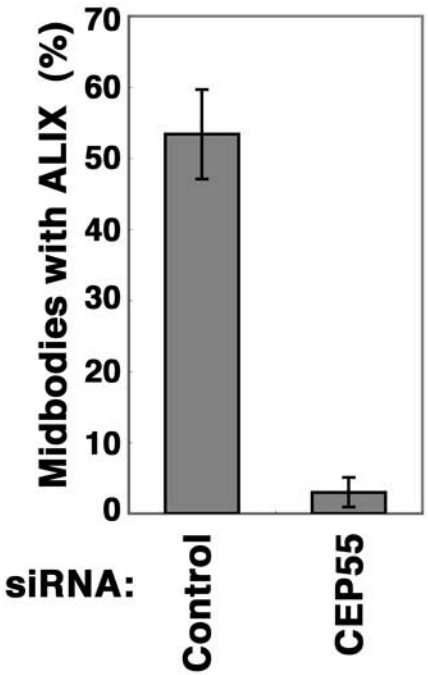

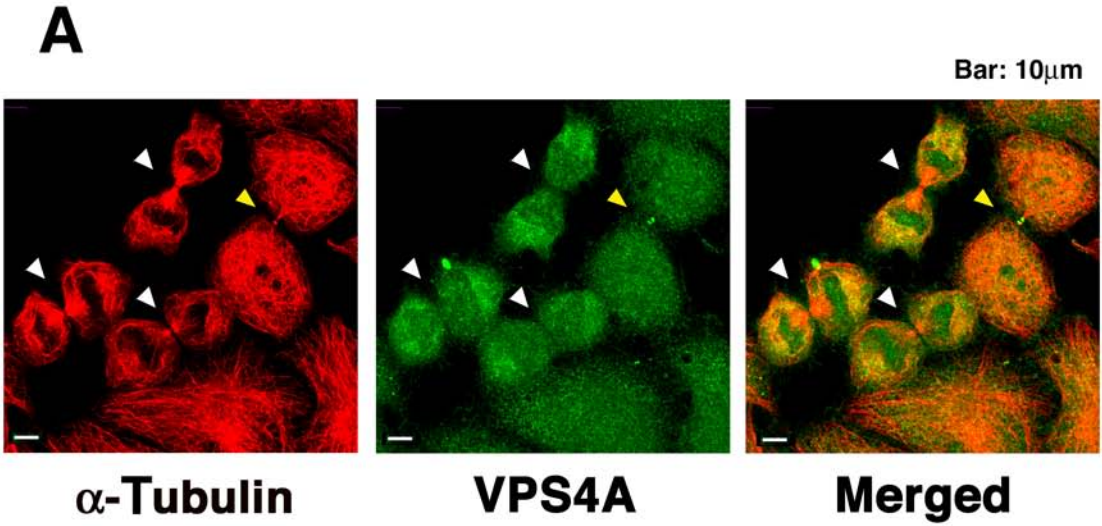
A
Bar: 10μm
α-Tubulin
VPS4A
Merged

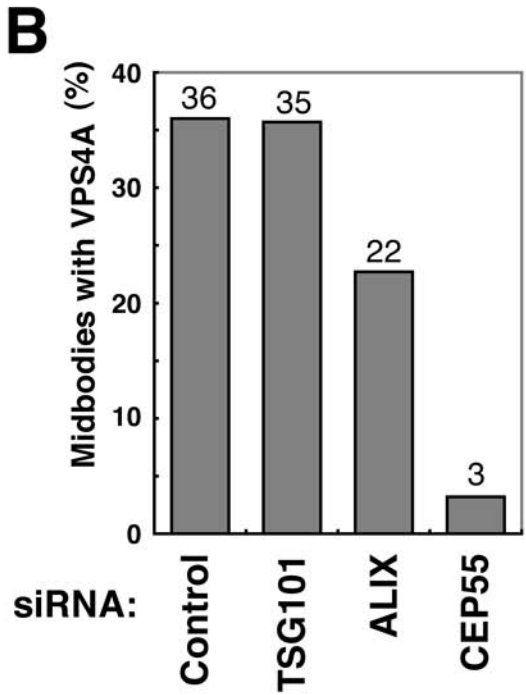
B
Midbodies with VPS4A (%)
40
30
20
10
0
36
35
22
3
siRNA:
Control
TSG101
ALIX
CEP55

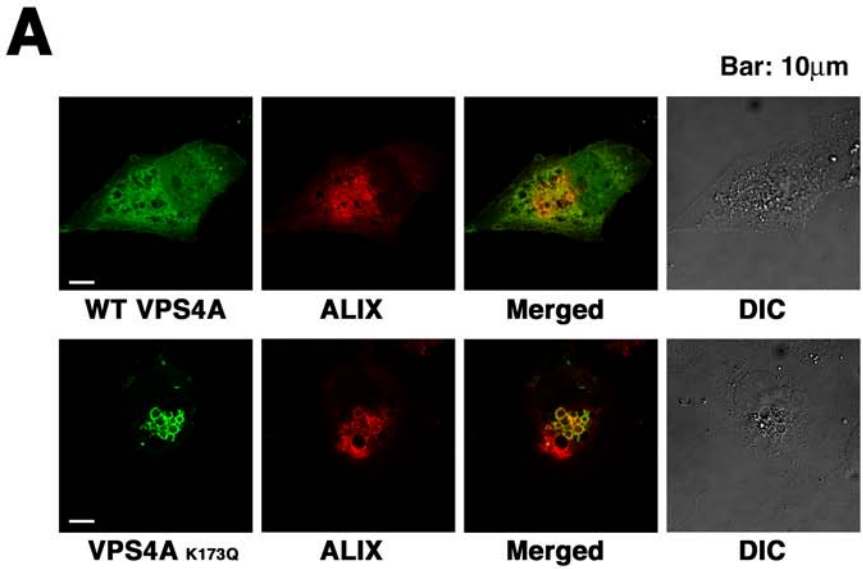
A
Bar: 10μm
WT VPS4A
ALIX
Merged
DIC
VPS4A K173Q
ALIX
Merged
DIC

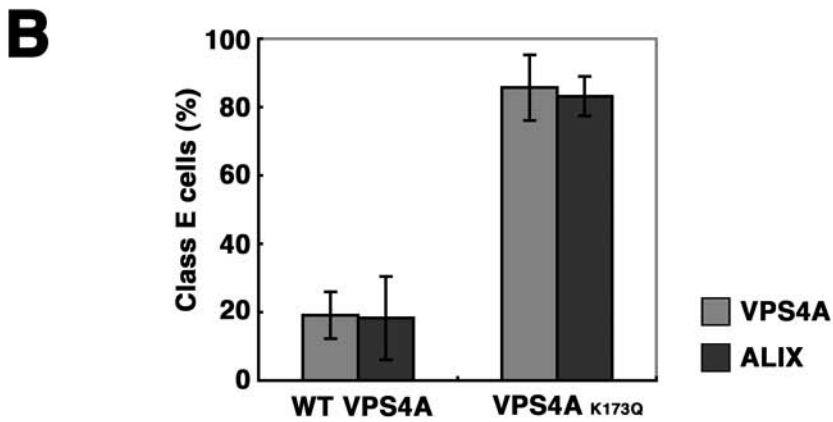
B
Class E cells (%)
100
80
60
40
20
0
WT VPS4A
VPS4A K173Q
VPS4A
ALIX